Drops climbing uphill on a slowly oscillating substrate

E. S. Benilov*
Department of Mathematics, University of Limerick, Limerick, Ireland
(Received 15 May 2010; published 27 August 2010)

We examine the dynamics of a two-dimensional drop on an inclined substrate vibrating vertically. The drop is assumed to be driven by its contact lines, while its shape is determined by a quasistatic balance of surface tension, gravity, and vibration-induced inertial force. It is shown that, if the dependence of the inertial force on time involves narrow/deep "troughs" and wide/low "plateaus," the drop can climb uphill. For thin drops, this conclusion is obtained analytically, whereas the general case is treated numerically. It is demonstrated that the nonlinear effects (associated with the large thickness of the drop) dramatically strengthen the drop's uphill motion.

DOI: 10.1103/PhysRevE.82.026320 PACS number(s): 47.55.D−, 47.55.nb

I. INTRODUCTION

Everyday experience suggests that, in the absence of a towel, the best way to remove liquid drops from an object is to shake it, so the drops would slide down and, eventually, fall off. In two recent papers, however, Brunet *et al.* [1,2] showed experimentally that, on a sloping substrate vibrating vertically, drops can actually climb uphill. Noblin *et al.* [3], in turn, examined drops on a horizontal substrate oscillating both vertically and horizontally and demonstrated that the mean velocity of the drop can be "tuned" to a given value by varying the phase shift between the two oscillations.

A possible explanation of this counterintuitive effect was put forward in Ref. [4], where it was shown that the drop's uphill motion can be caused by interaction of the odd and even oscillatory modes induced in the drop by the substrate's vibrations. Note that, according to the model proposed, drops can climb uphill only if the vibration-induced inertial acceleration exceeds gravity by an order of magnitude. This conclusion agrees with the experimental results: in those reported in Refs. [1,2], for example, the inertial acceleration was indeed up to $50g$. Note also that, in all of the above papers, both theoretical and experimental, the substrate oscillations were harmonic.

The present paper examines the effect of *nonharmonic* oscillations. It will be shown that, provided they have a certain shape (wide flat "crests" and narrow deep troughs), they can make the drop climb uphill even if the inertial acceleration is on the order of g.

To simplify the problem, we shall confine ourselves to two spatial dimensions and also adopt a quasistatic approximation (physically, the latter amounts to the assumption that the drop's shape is determined by the balance of surface tension, gravity, and the vibration-induced inertial force, while the drop's dynamics are driven by the contact lines). In Sec. II, we shall formulate the problem and, in Sec. III, examine asymptotically the limit of thin drops. Drops of arbitrary thickness will be examined numerically in Sec. IV.

II. FORMULATION OF THE PROBLEM

In what follows, we shall use the quasistatic approximation (QSA) to derive an equation for the drop's thickness (Sec. II A). In Sec. II B, we shall formulate the model describing the motion of the drop's contact lines and in Sec. II C the full set of the governing equations and boundary conditions.

A. Quasistatic approximation (QSA)

Consider a two-dimensional drop of liquid (of density ρ, kinematic viscosity ν, and surface tension σ) on a vibrating plate inclined at an angle α to the horizontal (see Fig. 1). We shall assume the plate's vibration to be strictly vertical, so the acceleration due to gravity g, whichever equation or boundary condition it appears in, can be replaced with an effective acceleration a due to both gravity and the vibration-induced inertial force.

Let the x axis of the (x,z) coordinate system be parallel to the plate. Then, the vector velocity (u,w) of the liquid and its pressure p satisfy the two-dimensional Navier-Stokes equations,

$$\frac{\partial u}{\partial t}+u\frac{\partial u}{\partial x}+w\frac{\partial u}{\partial z}+\frac{1}{\rho}\frac{\partial p}{\partial x}=-a\sin\alpha+\nu\left(\frac{\partial^2 u}{\partial x^2}+\frac{\partial^2 u}{\partial z^2}\right), \tag{1}$$

$$\frac{\partial w}{\partial t}+u\frac{\partial w}{\partial x}+w\frac{\partial w}{\partial z}+\frac{1}{\rho}\frac{\partial p}{\partial z}=-a\cos\alpha+\nu\left(\frac{\partial^2 w}{\partial x^2}+\frac{\partial^2 w}{\partial z^2}\right), \tag{2}$$

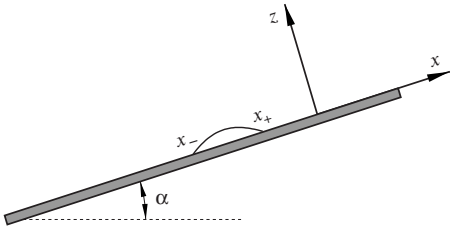

FIG. 1. The setting: a drop on an inclined substrate oscillating vertically.

*http://www.staff.ul.ie/eugenebenilov/hpage/; eugene.benilov@ul.ie

$$\frac{\partial u}{\partial x}+\frac{\partial w}{\partial z}=0, \tag{3}$$

where the acceleration a is due to both gravity and vibration-induced inertial force. The dynamic boundary conditions at the drop's free boundary, $z=h(x,t)$, are

$$\mathbf{n}\cdot\mathbf{Sn}=\sigma c, \quad \mathbf{t}\cdot\mathbf{Sn}=0 \quad \text{at } z=h, \tag{4}$$

where the unit normal and tangential vectors are given by

$$\mathbf{n}=\left[1+\left(\frac{\partial h}{\partial x}\right)^2\right]^{-1/2}\begin{bmatrix}\frac{\partial h}{\partial x}\\ 1\end{bmatrix}, \tag{5}$$

$$\mathbf{t}=\left[1+\left(\frac{\partial h}{\partial x}\right)^2\right]^{-1/2}\begin{bmatrix}1\\ -\frac{\partial h}{\partial x}\end{bmatrix}, \tag{6}$$

and the stress tensor and curvature are given by

$$\mathbf{S}=\rho\nu\begin{bmatrix}2\frac{\partial u}{\partial x}-\frac{p}{\rho\nu} & \frac{\partial u}{\partial z}+\frac{\partial w}{\partial x}\\ \frac{\partial u}{\partial z}+\frac{\partial w}{\partial x} & 2\frac{\partial w}{\partial z}-\frac{p}{\rho\nu}\end{bmatrix}, \tag{7}$$

$$c=\frac{\partial^2 h}{\partial x^2}\left[1+\left(\frac{\partial h}{\partial x}\right)^2\right]^{-3/2}. \tag{8}$$

It is convenient to decompose the pressure into the dynamic and hydrostatic parts (denoting the former by $\hat{p}$),

$$p=\hat{p}-\rho a(x\sin\alpha+z\cos\alpha). \tag{9}$$

We shall introduce the following dimensionless variables:

$$a_*=\frac{a}{A}, \quad x_*=\frac{x}{X}, \quad z_*=\frac{z}{H}, \quad t_*=\frac{t}{T}, \tag{10}$$

$$u_*=\frac{u}{U}, \quad w_*=\frac{w}{W}, \quad \hat{p}_*=\frac{\hat{p}}{\hat{P}}, \tag{11}$$

$$h_*=\frac{h}{H}, \quad c_*=\frac{c}{C}, \tag{12}$$

where T is the period of the plate's vibration; X and H are the drop's characteristic width and depth; and A, C, U, W, and $\hat{P}$ are the characteristic scales for a, c, u, w, and $\hat{p}$. Naturally, not all of these scales are independent: the curvature scale, for example, is related to the drop's width and depth by

$$C=\frac{H}{X^2}, \tag{13}$$

whereas the continuity equation implies

$$\frac{U}{X}=\frac{W}{H}, \tag{14}$$

and we shall also assume, as is customary in fluid dynamics,

$$U=\frac{X}{T}. \tag{15}$$

Finally, we are interested in the regimes where surface tension is at least one of the main effects, which implies

$$\hat{P}=\sigma C. \tag{16}$$

Substituting Eqs. (10)–(16) into Eqs. (1)–(9) and omitting the asterisks, we obtain

$$\lambda\left(\frac{\partial u}{\partial t}+u\frac{\partial u}{\partial x}+w\frac{\partial u}{\partial z}\right)+\frac{\partial \hat{p}}{\partial x}=\mu\left(\varepsilon^2\frac{\partial^2 u}{\partial x^2}+\frac{\partial^2 u}{\partial z^2}\right), \tag{17}$$

$$\lambda\varepsilon^2\left(\frac{\partial w}{\partial t}+u\frac{\partial w}{\partial x}+w\frac{\partial w}{\partial z}\right)+\frac{\partial \hat{p}}{\partial z}=\varepsilon^2\mu\left(\varepsilon^2\frac{\partial^2 w}{\partial x^2}+\frac{\partial^2 w}{\partial z^2}\right), \tag{18}$$

$$\frac{\partial u}{\partial x}+\frac{\partial w}{\partial z}=0, \tag{19}$$

$$\left[2\varepsilon^2\frac{\partial u}{\partial x}-\frac{\hat{p}-\beta a(x+\gamma h)+c}{\mu}\right]\frac{\partial h}{\partial x}+\frac{\partial u}{\partial z}+\varepsilon^2\frac{\partial w}{\partial x}=0 \quad \text{at } z=h, \tag{20}$$

$$\varepsilon^2\left(\frac{\partial u}{\partial z}+\varepsilon^2\frac{\partial w}{\partial x}\right)\frac{\partial h}{\partial x}+2\varepsilon^2\frac{\partial w}{\partial z}-\frac{\hat{p}-\beta a(x+\gamma h)+c}{\mu}=0 \quad \text{at } z=h, \tag{21}$$

$$c=\frac{\partial^2 h}{\partial x^2}\left[1+\varepsilon^2\left(\frac{\partial h}{\partial x}\right)^2\right]^{-3/2}, \tag{22}$$

where the parameters

$$\lambda=\frac{\rho X^4}{\sigma H T^2}, \quad \mu=\frac{\rho\nu X^4}{\sigma H^3 T}, \quad \beta=\frac{\rho X^3 A\sin\alpha}{\sigma H} \tag{23}$$

characterize the liquid's inertia, viscosity, and gravity (all relative to surface tension), and

$$\varepsilon=\frac{H}{X}, \quad \gamma=\frac{\varepsilon}{\tan\alpha} \tag{24}$$

are the drop's aspect ratio and the ratio of that to the substrate's slope.

In this work, we shall assume that

$$\lambda\ll 1, \quad \mu\ll 1,$$

whereas β, ε, and γ can be arbitrary. Note that the applicability of the QSA is not affected by the Reynolds number (equal to λ/μ), as it characterizes the strength of the liquid's inertia relative to viscosity, both of which are neglected and it is unimportant which one is stronger.

Now, neglecting small terms in Eqs. (17), (18), and (20)–(22) and omitting Eq. (19) altogether (as it will not be needed), we obtain

$$\frac{\partial \hat{p}}{\partial x} = 0, \quad \frac{\partial \hat{p}}{\partial z} = 0, \tag{25}$$

$$\hat{p} = \beta a(x + \gamma h) - \frac{\partial^2 h}{\partial x^2}\left[1 + \varepsilon^2\left(\frac{\partial h}{\partial x}\right)^2\right]^{-3/2} \quad \text{at } z = h. \tag{26}$$

It follows from Eq. (25) that $\hat{p}$ is independent of x and y; hence, it can be compatible with Eq. (26) only if

$$\frac{\partial}{\partial x}\left\{\beta a(x + \gamma h) - \frac{\partial^2 h}{\partial x^2}\left[1 + \varepsilon^2\left(\frac{\partial h}{\partial x}\right)^2\right]^{-3/2}\right\} = 0. \tag{27}$$

This equation reflects the balance of gravity or inertial force and surface tension (corresponding to the terms involving a and $\partial^2 h/\partial x^2$, respectively). Finally, note that an approximation similar to the QSA has been previously used (without a derivation) in Ref. [5] for shallow rivulets.

B. Motion of the contact lines

To describe the motion of the contact lines, we shall require, as usually done (e.g., Ref. [6]), that their velocities depend on the contact angles $\theta_{\pm}$,

$$\frac{dx_{\pm}}{dt} = \pm v(\theta_{\pm}), \tag{28}$$

where $x_{\pm}(t)$ are the coordinates of the contact lines and $v(\theta)$ is a given function (determined by the material properties of the liquid and substrate). We shall now discuss the dependence of the contact-line velocity v on the contact angle θ. For most liquid/substrate combinations, $v(\theta)$ involves a hysteresis interval (θ_r, θ_a) such that, for $\theta > \theta_a$, the contact line advances; for $\theta < \theta_r$, it recedes; and, for $\theta_r \le \theta \le \theta_a$, it is stationary. Accordingly, we assume

$$v = \begin{cases} -v_r|\theta - \theta_r|^{n_r} & \text{if } \theta < \theta_r \\ 0 & \text{if } \theta_r \le \theta \le \theta_a \\ v_a|\theta - \theta_a|^{n_a} & \text{if } \theta > \theta_a, \end{cases} \tag{29}$$

where v_r, v_a, n_r, and n_a are positive constants. Expression (29) should be viewed as an analytical approximation of the "real-life" dependence $v(\theta)$ near the hysteresis interval, as we shall not be interested in the ranges $\theta \ll \theta_r$ and $\theta_r \gg \theta_a$. Indeed, due to the oscillatory nature of the drop's evolution, its contact angles oscillate about an equilibrium value located inside the hysteresis interval; hence, we shall assume that the six adjustable constants involved in Eq. (29) are chosen to provide the best fit for the experimental $v(\theta)$ near the hysteresis interval.

We shall also consider the following particular case of Eq. (29):

$$v = v_0(\theta - \theta_0)^3, \tag{30}$$

where the hysteresis interval shrinks to a point, $\theta_a = \theta_r = \theta_0$. Relationship (30) involves only two adjustable parameters and, thus, cannot approximate the real-life dependence $v(\theta)$. We shall use it as a simple example to illustrate our approach.

Note that, everywhere in this paper, it is implied that θ is the *macroscopic* contact angle, i.e., measured outside the boundary layer caused by relaxation of the no-slip condition. It is well known [7,8] that this boundary layer can involve rapid bending of the drop's surface, so the *microscopic* contact angle (the one measured at the actual contact lines) can noticeably differ from θ.

C. Full set of governing equations and boundary conditions

Now, when our scaling analysis and parameter estimates have been carried out, it is convenient to redefine the scales H and X in such a way that

$$\beta = 1. \tag{31}$$

Then, substitution of Eq. (31) into Eq. (27) yields

$$\frac{\partial}{\partial x}\left\{\frac{\partial^2 h}{\partial x^2}\left[1 + \varepsilon^2\left(\frac{\partial h}{\partial x}\right)^2\right]^{-3/2} - \gamma a h\right\} = a. \tag{32}$$

Note that Eq. (31) does not introduce a new restriction, as we do not omit any terms because of it [and, in principle, the original Eq. (27) could be used instead].

The solution of Eq. (32) should also satisfy the (two-dimensional) mass conservation law. Assuming that the product of X and H equals the dimensional cross-sectional area of the drop (so the dimensionless one equals unity), we shall require

$$\int_{x_-}^{x_+} h dx = 1. \tag{33}$$

Next, by definition, contact lines are characterized by zero thickness of the drop, i.e., we should require

$$h = 0 \quad \text{at } x = x_{\pm}. \tag{34}$$

At any time t, given the current values of $x_{\pm}(t)$ and $a(t)$, the boundary-value problem (32)–(34) fully determines the drop's shape.

Next, introduce the drop's position x_0 and the width w of its base,

$$x_0 = \tfrac{1}{2}(x_+ + x_-), \quad w = x_+ - x_-.$$

Then, replacing in Eq. (28) $x_{\pm}$ with x_0 and w, we obtain

$$\frac{dw}{dt} = v(\theta_+) + v(\theta_-), \tag{35}$$

$$\frac{dx_0}{dt} = \frac{1}{2}[v(\theta_+) - v(\theta_-)]. \tag{36}$$

The sets of Eqs. (32)–(34) and Eqs. (35) and (36) describe the drop's shape and dynamics, respectively. They are coupled through the relationship of the contact angles $\theta_{\pm}(t)$ and the drop's shape $h(x,t)$,

$$\tan\theta_{\pm} = \mp \varepsilon\left(\frac{\partial h}{\partial x}\right)_{x=x_{\pm}}, \quad 0 \le \theta_{\pm} \le \pi. \tag{37}$$

Finally, let the acceleration scale A equal g. As a result—since the vibration-induced part of a has a zero mean—the

mean dimensionless acceleration must equal unity, i.e.,

$$\int_0^1 a dt = 1. \tag{38}$$

III. THIN DROPS

Let the drop under consideration have small aspect ratio, $H \ll X$, i.e.,

$$\varepsilon \ll 1.$$

In this case, the problem can be examined asymptotically through a thin-drop approximation.

In order to clarify when the QSA is applicable to our problem, note that drops on a vibrating substrate are expected to evolve periodically, which implies that their contact angles oscillate about some equilibrium values located within the hysteresis interval. As a result, the QSA is applicable when the hysteresis interval is located in the region of small θ, i.e., the liquid under consideration is close to being perfectly wetting.

To understand the advantages of the thin-drop approximation, recall that our governing equations can be subdivided into two subsets: the boundary-value problem (32)–(34) for the drop's shape and the initial-value problem (35) and (36) for the evolution of the drop's width and position. The thin-drop approximation enables one to solve the former and, thus, find explicit expressions for the contact angles $\theta_\pm$ as functions of the drop's width w. These expressions can then be substituted into the latter (initial-value) problem, making it much easier to analyze and/or simulate.

Next, recall that the parameter γ [defined by Eq. (24)] involves ε and, hence, is affected by the assumption $\varepsilon \ll 1$. Accordingly, two thin-drop regimes can be distinguished: one, where the substrate's slope $\tan\alpha$ is of order 1; hence,

$$\gamma \ll 1,$$

and another regime, where $\tan\alpha \sim \varepsilon$—in which case,

$$\gamma \sim 1.$$

These regimes are examined in the following two sections.

A. Case of order-1 slope of the substrate ($\gamma \ll 1$)

Omitting the terms involving ε and γ from Eq. (32), we obtain

$$\frac{\partial^3 h}{\partial x^3} = a, \tag{39}$$

which yields

$$h = \tfrac{1}{6} a x^3 + C_1 x^2 + C_2 x + C_3, \tag{40}$$

where the constants of integration C_1, C_2, and C_3 depend, generally, on the time t. Substituting Eq. (40) into Eqs. (33) and (34), we obtain

$$\tfrac{1}{24} a(x_+^4 - x_-^4) + \tfrac{1}{3} C_1 (x_+^3 - x_-^3) + \tfrac{1}{2} C_2 (x_+^2 - x_-^2) + C_3 (x_+ - x_-) = 1, \tag{41}$$

$$\tfrac{1}{6} a x_\pm^3 + C_1 x_\pm^2 + C_2 x_\pm + C_3 = 0. \tag{42}$$

Solving Eqs. (41) and (42) for $C_{1,2,3}$, substituting them into Eqs. (40) and (37), and assuming $|\theta_\pm| \ll 1$ (hence, replacing $\tan\theta_\pm$ with $\theta_\pm$), we obtain

$$\theta_\pm = \varepsilon \left(\frac{6}{w^2} \mp \frac{a w^2}{12} \right), \tag{43}$$

where, as before, $w = x_+ - x_-$ is the width of the drop's base. Observe that, expectedly, $\theta_\pm$ do not depend on the drop's position x_0; hence, Eqs. (35) and (43) form a "closed" equation for w.

First we shall consider the simplest example of $v(\theta)$, i.e., Eq. (30)—in which case, Eq. (35) becomes

$$\frac{dw}{dt} = 2 v_0 \varepsilon^3 \left[\left(\frac{6}{w^2} - \frac{\theta_0}{\varepsilon} \right)^3 + 3 \left(\frac{6}{w^2} - \frac{\theta_0}{\varepsilon} \right) \left(\frac{a w^2}{12} \right)^2 \right].$$

This equation has a steady solution,

$$w = \sqrt{\frac{6\varepsilon}{\theta_0}}, \tag{44}$$

i.e., the drop's width remains constant (but its shape is still variable, as it depends on the acceleration a which changes in time). Upon substitution of Eq. (44) into Eq. (36), we obtain

$$\frac{dx_0}{dt} = -\frac{v_0 \varepsilon^6 a^3}{8 \theta_0^3}. \tag{45}$$

Note that the equilibrium angle is implied to be small here, $\theta_0 \sim \varepsilon$; otherwise, the thin-drop approximation (used to obtain all of the above results) becomes inapplicable.

Now, recall that $a(t)$ is periodic and nondimensionalized in such a way that its period equals unity. Then, if

$$\int_0^1 a^3 dt < 0, \tag{46}$$

the solution $x_0(t)$ of Eq. (45) grows with time, i.e., *the drop climbs uphill*.

Recall also that, dimensionally, the acceleration due to gravity or inertia satisfies restriction (3), the dimensionless equivalent of which is

$$\int_0^1 a dt = 1 \tag{47}$$

(where the unity on the right-hand side is the dimensionless equivalent of g). An obvious example of $a(t)$ satisfying condition Eq. (47) is

$$a(t) = 1 + A \sin 2\pi t,$$

where A is a constant—which, however, does not satisfy Eq. (46) and, thus, cannot make the drop climb uphill. The same applies to any $a(t)$ with symmetric crests and troughs.

In fact, Eqs. (46) and (47) can hold simultaneously only if $a(t)$ involves wide/low crests (or rather plateaus) and narrow/deep troughs. Consider, for example, piecewise-constant acceleration,

$$a(t) = 1 + \begin{cases} a_1 & \text{if } 0 \le t < t_1 \\ -a_2 & \text{if } t_1 \le t < 1, \end{cases} \tag{48}$$

where $a_{1,2} > 0$ and $t_1 < 1$ are constants. In this case, condition (47) implies

$$t_1 = \frac{a_2}{a_1 + a_2},$$

whereas condition (46) holds if

$$\frac{(a_2 - 1)^3}{a_2} > \frac{(a_1 + 1)^3}{a_1},$$

and it can be readily shown that the two conditions can hold simultaneously only if

$$a_2 > a_1, \quad t_1 > \tfrac{1}{2}.$$

In other words, thin drops can climb uphill only if the downward acceleration is stronger than the upward one, but the latter acts during more than half of the period.

We shall now discuss to which extent our conclusions depend on the specific form of the dependence of the contact-line velocity on the contact angle, $v(\theta)$. First of all, observe that, even though the steady solution (44) was obtained for the particular case (30), it actually satisfies Eq. (35) for *any* $v(\theta)$, for which θ_0 exists such that

$$v(\theta_0 - \theta) = -v(\theta_0 + \theta) \quad \text{for all } \theta.$$

In what follows, such $v(\theta)$ will be referred to as antisymmetric (with respect to θ_0). For an antisymmetric $v(\theta)$, criterion (46) can be readily generalized,

$$\int_0^1 \left[v\left(\theta_0 - \frac{\varepsilon a}{2\theta_0}\right) - v\left(\theta_0 + \frac{\varepsilon a}{2\theta_0}\right) \right] dt < 0, \tag{49}$$

which is, essentially, the condition of whether or not (thin) drops climb uphill for a given acceleration $a(t)$ and antisymmetric $v(\theta)$.

We have also considered examples of nonantisymmetric $v(\theta)$, both with and without hysteresis intervals. In this case, the width w of the drop's base depends on t, so Eq. (3) does not have an obvious analytical solution. It can still be solved numerically (using, say, the Runge-Kutta algorithm), and a typical behavior is illustrated in Fig. 2(a). One can see that $w(t)$ oscillates with the frequency of the substrate's vibration and, at the same time, slowly drifts toward a certain mean value. For a particular case of $v(\theta)$ given by Eq. (29) with $n_a = n_r = n$, it can be shown analytically that the amplitude of the oscillations and the time scale of the drift are $O(\varepsilon^n)$ and $O(\varepsilon^{-2n})$, respectively. We shall not discuss further features of the asymptotic solutions, as they are sensitive to the specific form of $v(\theta)$ and $a(t)$.

Overall, several dozens of examples of $v(\theta)$ and $a(t)$ have been examined numerically. In all cases, without a single exception, if the troughs of $a(t)$ were sufficiently narrow and deep, the drop would climb uphill.

B. Discussion

In this section, we shall discuss the qualitative aspects of the above explanation of the effect of climbing drops. First of all, observe that, if $v(\theta)$ is a linear function, it can be verified that Eq. (49) does not hold for *any* $a(t)$. We conclude that drops can climb uphill only if the dependence of the contact-line velocity on the contact angle is nonlinear.

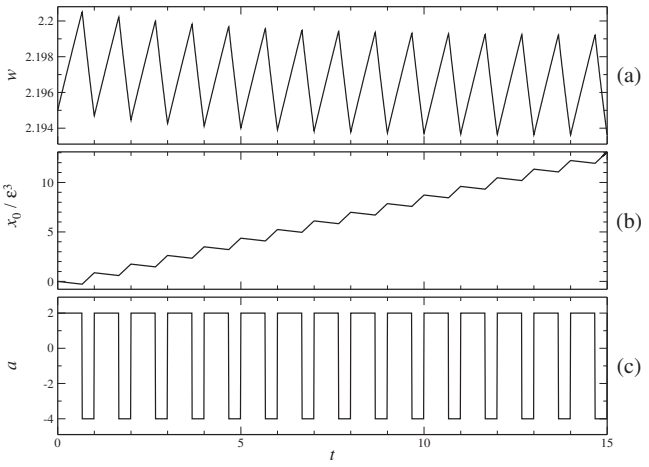

FIG. 2. A thin drop's evolution, for $\varepsilon = 0.3$ and $\gamma = 0$. $v(\theta)$ is given by Eq. (29) with $v_r = 1.5$, $v_a = 0.5$, $n_r = n_a = 3$, and $\theta_r = \theta_a = \varepsilon$. $a(t)$ is given by Eq. (48) with $a_1 = 2$, $a_2 = 4$, and $t_1 = \frac{5}{6}$. (a) The width of the drop's base $w(t)$, (b) the drop's displacement $x_0(t)$, and (c) the acceleration $a(t)$.

Generally, drop's velocity depends on the velocities $v_\pm$ of its contact lines—which, in turn, depend on the contact angles $\theta_\pm$—and those, eventually, depend on the effective gravity a. Furthermore, the dependence of $v_\pm$ on a "preserves signs"—i.e., when $a > 0$, the contact lines slide down, and when $a < 0$ they climb uphill. Clearly, the drop as a whole behaves in a similar manner.

Note, however, that the dependence of $v_\pm$ on $\theta_\pm$ is, generally, *nonlinear*—and so is, consequently, the dependence of the drop's velocity on the acceleration a. As a result, the drop's mean displacement (per period of vibration) does not necessarily have the same sign as the mean a.

In other words, the effect of climbing drops observed in the present model is of kinematic nature and is due to the nonlinearity of the dependence of the contact-line velocity on the contact angle. Note also that all examples of $v(\theta)$ that involve a hysteresis interval are nonlinear by definition; hence, given an appropriate $a(t)$, drops can climb uphill.

Finally, we mention Ref. [9] which examined drops on a horizontal substrate oscillating tangentially. In this case, a similar kinematic effect was observed: even though the mean acceleration of the substrate was zero, the drops were observed drifting in a direction determined by the asymmetries of the vibration (similar to the effect examined in this paper).

C. Limit of small slope of the substrate ($\gamma \sim 1$)

Definition (24) of γ shows that, for a given drop (hence, given ε), an increase in γ corresponds to a decrease in the substrate's slope. As a result, the effect of gravity becomes weaker, making it easier for the drop to climb uphill.

To validate the above conclusion, assume that $\varepsilon \ll 1$, but $\gamma \sim 1$. Omitting, accordingly, the term involving ε from Eq. (32), but keeping the one with γ, we obtain

$$\frac{\partial^3 h}{\partial x^3} - \gamma a \frac{\partial h}{\partial x} = a.$$

This is the finite-γ equivalent of Eq. (39), with the rest of the governing set being the same as that for the limit $\gamma \ll 1$ examined previously. Then, expressing the contact angles in terms of the drop's width and acceleration, we obtain

$$\theta_{\pm} = \begin{cases} \varepsilon \left[\dfrac{\gamma^2 a(\cosh \hat{w} - 1) \mp \frac{1}{2}\hat{w}^2(\cosh \hat{w} + 1) \pm \hat{w} \sinh \hat{w}}{\gamma(\hat{w} \sinh \hat{w} - 2 \cosh \hat{w} + 2)} \pm \dfrac{1}{\gamma} \right] & \text{if } a \geq 0 \\ \varepsilon \left[\dfrac{\gamma^2 a(\cos \hat{w} - 1) \mp \frac{1}{2}\hat{w}^2(\cos \hat{w} + 1) \mp \hat{w} \sin \hat{w}}{\gamma(-\hat{w} \sin \hat{w} - 2 \cos \hat{w} + 2)} \pm \dfrac{1}{\gamma} \right] & \text{if } a < 0, \end{cases} \tag{50}$$

where $\hat{w} = \sqrt{\gamma |a|}\, w$.

Unlike the small-γ limit, the present case does not admit any obvious exact solution [11]. Still, Eqs. (35), (36), and (50) can be readily simulated numerically. A typical set of numerical results is shown in Fig. 3: one can see that increasing γ (i.e., decreasing the substrate's slope) does make the drops climb faster. Moreover, for a finite γ, this effect can be observed even if condition (46) does *not* hold [mathematically, this does not pose a contradiction, as Eq. (46) was derived for $\gamma = 0$].

It should be emphasized, however, that, if one gradually "symmetrizes' the acceleration's inertial part, the drop will, sooner or later, start sliding downhill. In order to illustrate this conclusion, the drop's evolution was computed for the piecewise-constant model (48) with

$$a_1 = 1, \quad a_2 = 5, \quad t_1 = \frac{5}{6} \quad \left(\int_0^1 a^3 dt = -4 \right), \tag{51}$$

$$a_1 = 1, \quad a_2 = 4, \quad t_1 = \frac{4}{5} \quad \left(\int_0^1 a^3 dt = +1 \right), \tag{52}$$

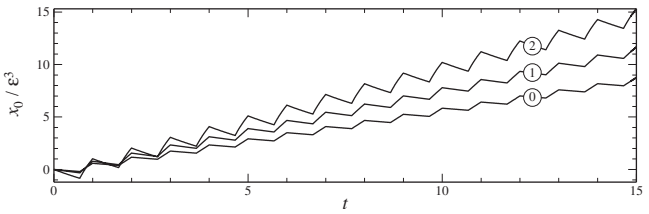

FIG. 3. A thin drop's position $x_0(t)$ for $\varepsilon = 0.3$ and increasing values of γ. $v(\theta)$ is given by Eq. (30) with $v_0 = 1$ and $\theta_0 = \frac{3}{2}\varepsilon$. $a(t)$ is the same as in Fig. 2. The curves are marked with the corresponding value of γ.

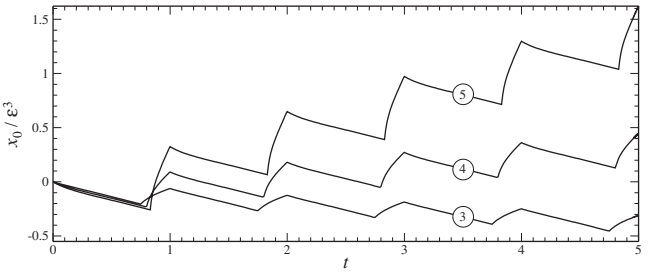

FIG. 4. A thin drop's position $x_0(t)$ for $\gamma = 1$ and the same $v(\theta)$ as in Fig. 3. $a(t)$ is given by Eq. (48) with parameters (51)–(53). The curves are marked with the corresponding values of a_2.

$$a_1 = 1, \quad a_2 = 3, \quad t_1 = \frac{3}{4} \quad \left(\int_0^1 a^3 dt = +4 \right). \tag{53}$$

The results are shown in Fig. 4: one can see that the drop started to slide downhill well before the inertial part of $a(t)$ would become fully symmetric.

IV. GENERAL CASE

In the case where the slope of the drop's surface is of order 1 ($\varepsilon \sim 1$), the problem does not involve small parameters and, thus, has to be examined numerically. Note also that, for finite ε, the drop can evolve in such a way that $\partial h / \partial x$ becomes infinite at certain points, while h becomes a multivalued function of x (e.g., two different values of h correspond to the same x). Such a situation occurs, for example, when the drop's base becomes narrower than its maximum width.

Thus, the boundary-value problem (32)–(34) (describing the drop's shape) needs to be rewritten in terms of variables that would remain regular even if h becomes multivalued. These variables are described in the Appendix. Then, to simulate the evolution of the drop, problem (32)–(34) should be solved for a given width w of the drop at every time step (using the numerical method described in the Appendix), and the resulting values of $\theta_{\pm}$ are to be "fed" into the right-hand sides of Eqs. (35) and (36) for w and x_0. Note that such an approach is more cumbersome than that in the case of thin drops (where $\theta_{\pm}$ could be related to w analytically).

As before, we have considered a large number of examples of $v(\theta)$ and $a(t)$. In particular, continuous (and, thus, more realistic than piecewise-constant) examples of $a(t)$ were examined, such as

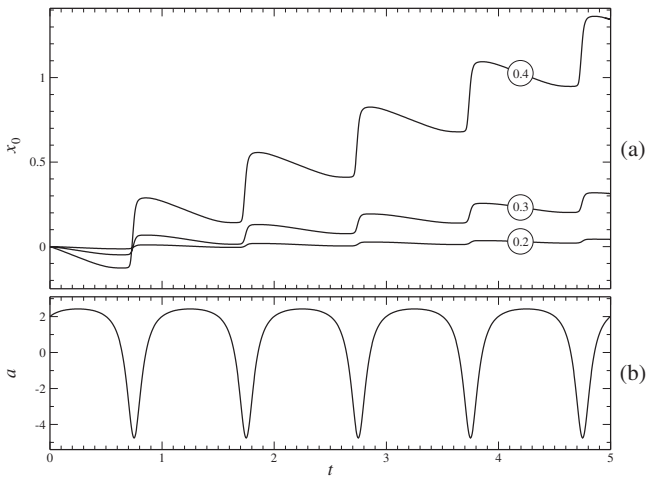

FIG. 5. The evolution of drops with order-1 ε. The curves are marked with the corresponding values of ε^2. In all cases, $\gamma=0$, $v(\theta)$ is determined by Eq. (30) with $v_0=1$ and $\theta_0=1$, and $a(t)$ is determined by Eqs. (54) and (55). (a) The drop's displacement $x_0(t)$ and (b) the acceleration $a(t)$.

$$a(t) = 1 + A\left(\frac{1}{\sqrt{B^2-1}} - \frac{1}{B+\sin 2\pi t}\right), \tag{54}$$

where A and B are constants [12]. Observe that, if $B \gg 1$, Eq. (54) tends to a function with symmetric crests and troughs, whereas the limit $B \to 1^+$ makes the crests wider and the troughs deeper. An example of $a(t)$ determined by Eq. (54) is shown in Fig. 5(b).

Generally, the main conclusion of this section is that the large-slope (nonlubrication) effects dramatically strengthen the effect of climbing drops: this tendency was observed for all values of γ and regardless of the specific dependences $v(\theta)$ and $a(t)$ used in the simulations. A typical behavior of a drop is shown in Fig. 5(a) for $a(t)$ given by Eq. (54) with

$$A = 1, \quad B = 1.130\,82 \quad \left(\int_0^1 a^3 dt \approx 0\right). \tag{55}$$

Observe that, since the mean value of a^3 in this example is zero, thin drops would neither climb uphill nor slide downhill—but those with a finite ε do climb uphill (see Fig. 5).

Note also that, even for a relatively low value of $\varepsilon^2=0.4$, the drop's shape differs dramatically from that predicted by the thin-drop approximation; in particular, h can become multivalued (as illustrated in Fig. 6). We conclude that, quantitatively, the nonlinear effects (associated with the drop being thick) play an important role in the problem at hand.

V. DISCUSSION AND CONCLUDING REMARKS

In this work, we have examined the evolution of a drop on a vibrating substrate, under the assumption that the drop's shape is determined by the balance of surface tension, gravity, and the vibration-induced inertial force—while its dynamics are driven by the contact lines. First, we assumed

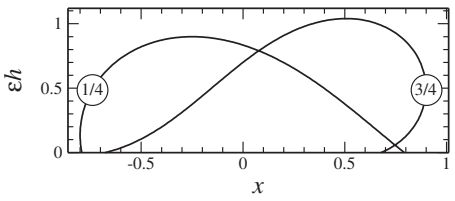

FIG. 6. "Snapshots" of the drop with $\varepsilon^2=0.4$, at the moments of extreme acceleration: maximum upward acceleration (occurs at a quarter of the period, $t=\frac{1}{4}$) and maximum downward acceleration ($t=\frac{3}{4}$). The curves are marked with the corresponding values of t. All parameters are the same as in Fig. 5.

$$\varepsilon \ll 1, \quad \gamma \ll 1, \tag{56}$$

where ε and γ are the characteristic slope of the drop's surface and the ratio of that to the substrate's slope [see Eq. (24)]. The former of conditions (56) enables one to take advantage of the thin-drop approximation, which considerably simplifies the analysis. Then, for the case where the dependence of the contact-line velocity v on the contact angle θ is antisymmetric, criterion (49) was derived, separating the cases where drops climb uphill or slide downhill. It turned out that the former occurs when, generally, the acceleration $a(t)$ (due to gravity and vibration-induced inertia) involves deep/narrow troughs and wide/low plateaus. For nonantisymmetric $v(\theta)$, no analytical criteria could be derived, but numerical simulations suggest that the drop's behavior is still determined by the structure of $a(t)$: if its maxima are sufficiently flat and its minima are deep, drops climb uphill. This is the first of the two main conclusions of this paper.

Most importantly, even though the applicability of limit (56) is restricted to thin drops, it supplies a "foothold" for tackling the general case—which can then be examined by gradually increasing ε and γ. Moreover, Eq. (56) provides the most conservative (and, hence, the safest) criterion of whether the drops can climb uphill, as any departure from it (through an increase in either ε or γ) enhances this effect. This is the second main conclusion of this paper.

We reiterate that the present work did not target quantitative agreement with the experimental results of Refs. [1,2] [the absence of measurements of $a(t)$ alone makes it impossible]. We rather propose a different experiment, where the inertial part of the acceleration is asymmetric—in which case the effect of climbing drops should be observable for much smaller amplitudes and frequencies of the vibration.

ACKNOWLEDGMENTS

The author is grateful to Jens Eggers and Stephen O'Brien for helpful discussions, and also acknowledges the support of the Science Foundation Ireland (RFP Grant No. 08/RFP/MTH1476 and Mathematics Initiative Grant No. 06/MI/005)

APPENDIX: ALTERNATIVE FORM OF THE BOUNDARY-VALUE PROBLEM (32)–(34)

Let ℓ be the arclength, i.e., the distance along the drop's surface. In what follows it will replace x as the free coordi-

nate, whereas x will be treated as an unknown alongside h. It is also convenient to introduce the angle Θ between the tangent to the drop's surface and the horizontal; it can be shown that

$$\frac{\partial x}{\partial \ell} = \cos\Theta, \quad \frac{\partial h}{\partial \ell} = \frac{\sin\Theta}{\varepsilon}. \tag{A1}$$

It can also be shown [10] that Eq. (32) can be rewritten in the form

$$\frac{\partial^2 \Theta}{\partial \ell^2} = a(\gamma \sin\Theta + \varepsilon \cos\Theta). \tag{A2}$$

Finally, the integral/boundary conditions (33) and (34) become

$$h = 0, \quad x = x_- \quad \text{at} \quad \ell = 0, \tag{A3}$$

$$h = 0, \quad x = x_+ \quad \text{at} \quad \ell = \ell_+, \tag{A4}$$

$$\int_0^{\ell_+} h \cos\Theta d\ell = 1, \tag{A5}$$

where ℓ_+ is the full length of the drop's surface (unknown *a priori*). Given the positions $x_\pm$ of the contact lines and the acceleration a, Eqs. (A1)–(A5) fully determine $x(\ell)$, $h(\ell)$, $\Theta(\ell)$, and ℓ_+. Once it is solved, the contact angles can be "collected" from $\Theta(\ell)$ through

$$\theta_- = \Theta(0), \quad \theta_+ = -\Theta(\ell_+).$$

In the present work, the boundary-value problem (A1)–(A5) was solved numerically using the shooting method. The unknowns to be determined through shooting were ℓ_+, θ_-, and the derivative of Θ at $\ell=0$ (in what follows, it will be denoted by Θ_0').

Given a set of values $(\ell_+, \theta_-, \Theta_0')$, the solution of Eqs. (A1) and (A2) was "shot" from $\ell=0$ toward $\ell=\ell_+$ subject to

$$\left.\begin{array}{ll} h = 0, & x = x_- \\ \Theta = \theta_-, & \dfrac{\partial\Theta}{\partial\ell} = \Theta_0' \end{array}\right\} \quad \text{at} \quad \ell = 0. \tag{A6}$$

Then ℓ_+, θ_-, and Θ_0' where iterated (through Newton's method) until conditions (A4) and (A5) held.

[1] P. Brunet, J. Eggers, and R. D. Deegan, Phys. Rev. Lett. **99**, 144501 (2007).
[2] P. Brunet, J. Eggers, and R. D. Deegan, Eur. Phys. J. Spec. Top. **166**, 11 (2009).
[3] X. Noblin, R. Kofman, and F. Celestini, Phys. Rev. Lett. **102**, 194504 (2009).
[4] E. S. Benilov and J. Billingham (unpublished).
[5] J. S. Sullivan, S. K. Wilson, and B. R. Duffy, Q. J. Mech. Appl. Math. **61**, 25 (2008).
[6] E. B. Dussan V., Annu. Rev. Fluid Mech. **11**, 371 (1979).
[7] O. V. Voinov, Fluid Dyn. **11**, 714 (1976).
[8] R. G. Cox, J. Fluid Mech. **168**, 169 (1986).
[9] S. Daniel, M. K. Chaudhury, and P.-G. de Gennes, Langmuir **21**, 4240 (2005).
[10] S. B. G. O'Brien, J. Fluid Mech. **233**, 519 (1991).
[11] Observe that the small-γ expression (43) has the form $\theta_\pm = f_1(W) \mp f_2(a, W)$, which was crucial for deriving the exact solution (44) for an antisymmetric $v(\theta)$. The finite-γ expression (50) is not representable in this form.
[12] The coefficients in expression (54) have been adjusted in such a way that, for all A and $B>1$, Eq. (54) has unit mean as required by condition (47).